

AD-A201 552

# Atomic structure of a {001} surface of Ni<sub>3</sub>Al

D. Sondericker and F. Jona

College of Engineering and Applied Science, State University of New York at Stony Brook, Stony Brook, New York 11794

P. M. Marcus

IBM Research Center, P.O. Box 218, Yorktown Heights, New York 10598

(Received 22 August 1985)

A low-energy electron diffraction intensity analysis of a clean Ni<sub>3</sub>Al{001} surface confirms the mixed-layer (50% Ni–50% Al) termination of this surface and reveals a small contraction of 2.8% of the first interlayer spacing (bulk value 1.78 Å), with the Al atoms slightly farther out (0.02 ± 0.03 Å) than the Ni atoms, while the second interlayer spacing is bulklike.

## I. INTRODUCTION

In a previous short publication<sup>1</sup> we reported the preliminary results of a low-energy electron diffraction (LEED) analysis of the structure of a clean Ni<sub>3</sub>Al{001} surface and a first-principles calculation of the relative stability of the two bulk terminations that are possible on such a surface. Ni<sub>3</sub>Al has the Cu<sub>3</sub>Au structure. In one of the {001} terminations the top atomic layer has a 50% Ni–50% Al composition (mixed layer); in the other termination, the composition of the top layer is 100% Ni (see Fig. 1). The

LEED analysis, based on visual evaluation of the fit between experiment and theory, produced unambiguous evidence in favor of the mixed-layer termination. A first-principles calculation of the cohesive energies of three-layer slabs found a larger cohesive energy for a slab with mixed-layer outer layers, suggesting that the mixed-layer surface is more stable, in accordance with the LEED results.

In this report we present the results of a quantitative refinement of the LEED intensity analysis based on minimization of reliability (*r*) factors with respect to the first and the second interlayer spacing and with respect to the relative positions of Al and Ni atoms (buckling) in the top atomic layer. The results are that the first interlayer spacing *d*<sub>12</sub> is contracted by 0.05 Å (or 2.8% of the bulk value 1.78 Å), the second interlayer spacing *d*<sub>23</sub> is bulklike, and in the top layer the Al atoms appear to be displaced very slightly (0.02 Å) outwards with respect to the Ni atoms. We present in Sec. II a few experimental details, in Sec. III the LEED intensity analysis, and in Sec. IV the conclusions.

## II. EXPERIMENTAL DETAILS

A large grain with suitable {001} orientation was identified by means of Laue patterns within, and cut by means of a spark cutter from, a polycrystalline ingot of Ni<sub>3</sub>Al. The surface to be studied (approximately 2 × 2 mm<sup>2</sup>) was oriented within 0.5° along {001}, lapped, and finally polished with 0.05-μm alumina slurry. Cleaning of the surface in the vacuum system was done with several cycles of Ar-ion bombardments (5 × 10<sup>-5</sup> Torr, 375 eV, ions incident at 45° to the surface, sample at room temperature, approximately 1 h/cycle) followed by one-hour anneals at 900°C. The sample was supported by a 0.05-mm-thick Ta foil and heated through this foil by electron bombardment. Auger electron spectroscopy (AES) in the retarding-grid mode (3000 eV primary energy, 5 eV modulation) was used to monitor the presence of impurities on the surface. The major impurities present before the cleaning process were sulfur, oxygen, and carbon. Sulfur was eliminated in 5 cleaning cycles; oxygen and carbon were depleted but still present in trace amounts

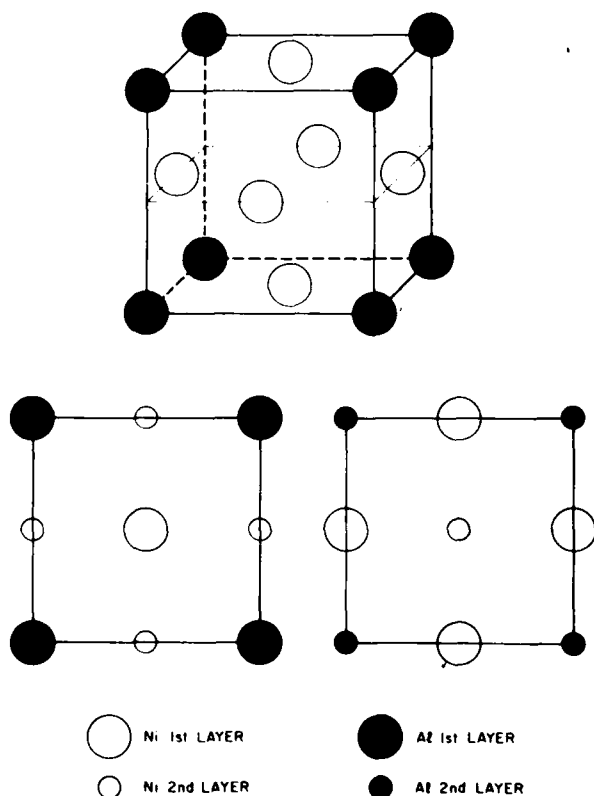


FIG. 1. Perspective view of the bulk unit cell of Ni<sub>3</sub>Al (top) and top views of the mixed-layer termination (bottom left) and of the Ni termination (bottom right) on {001}.

even after 15 cycles. The last two anneals prior to the collection of LEED intensity data were done at 700°C to minimize outgassing.

AES was also used to monitor the chemical composition and the relative stability of the surface during the cleaning and data-collecting processes. For these purposes the modulating voltage was reduced to 2 V in order to resolve the *KLL* Ni and Al peaks at 61 and 68 eV, respectively. The intensity ratio  $R_A = I(\text{Al}, 68 \text{ eV})/I(\text{Ni}, 61 \text{ eV})$  of these peaks was measured<sup>2</sup> immediately after an ion-bombardment cycle and then after a series of ten-minute anneals at increasing temperatures. Figure 2 shows the results typical of such annealing runs.  $R_A$  is about 0.6 after surface bombardment and increases monotonically to about 0.95 after annealing at 700°C, remaining constant at the latter value both for anneals at 800°C and after cooling to room temperature. These results indicate that (a) Al is preferentially sputtered from the surface, which is therefore Ni rich after argon-ion bombardment, and (b) the surface composition is stable after anneals at 700–800°C. It is this surface that was subjected to the LEED experiment.

The LEED pattern exhibited very sharp spots above a low background—indicative of a well-ordered, low-defect surface. The intensity data were collected with a computer-controlled television-camera system<sup>3</sup> and reduced to 3 sets of curves at 3 angles of incidence for a total of 45 LEED spectra (24 nondegenerate): 15 (4) at  $\theta=0^\circ$ ; 14 (9) at  $\theta=15.5^\circ$ ;  $\phi=-45^\circ$ ; 16 (11) at  $\theta=13.5^\circ$ ,  $\phi=0^\circ$ . For the definitions of  $\theta$  and  $\phi$  see, e.g., Ref. 4. All curves were normalized to constant incident current, the energy scale was corrected for the contact-potential difference between the electron-gun cathode and the sample (3.2 eV), and a uniform background was subtracted.

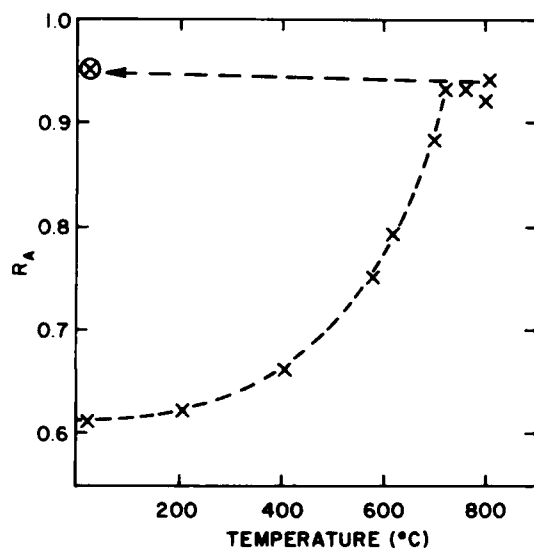


FIG. 2. Ratio  $R_A$  (defined in Ref. 2) of the Al and Ni AES peaks at 68 and 61 eV, respectively, from Ni<sub>3</sub>Al{001} after argon-ion bombardment (lowest value) and successive annealing treatments. For each cross on the curve, the heating current was raised, held for 10 min. and then  $R_A$  was measured.

TABLE I.  $r$ -factor values and energy ranges ( $\Delta E$ ) for all beam spectra measured experimentally on Ni<sub>3</sub>Al{001} as compared to calculations for the final model described in the text.

Beam	$r$ factor	$\Delta E$ (eV)
$\theta=0^\circ$		
$\bar{1}0$	0.0840	157
$0\bar{1}$	0.0974	163
$\bar{1}\bar{1}$	0.1278	138
$\bar{1}1$	0.1432	161
$1\bar{1}$	0.0766	143
20	0.1416	108
02	0.1260	121
$2\bar{0}$	0.1199	101
$0\bar{2}$	0.1119	101
$\bar{1}2$	0.0928	76
$2\bar{1}$	0.0585	73
$2\bar{1}$	0.0732	63
$2\bar{1}$	0.0623	72
$1\bar{2}$	0.1176	68
$\bar{1}\bar{2}$	0.0885	68
mean	0.1048	1613
$\theta=15.5^\circ$ , $\phi=-45^\circ$		
00	0.0855	158
$\bar{1}0$	0.0531	129
01	0.0762	137
10	0.2304	89
$0\bar{1}$	0.2516	88
11	0.1444	147
$\bar{1}\bar{1}$	0.0546	114
$2\bar{0}$	0.2781	132
$2\bar{1}$	0.1531	69
12	0.1497	107
$3\bar{3}$	0.1992	49
$3\bar{2}$	0.5608	69
30	0.4243	84
$3\bar{1}$	0.2677	103
mean	0.1854	1476
$\theta=13.5^\circ$ , $\phi=0^\circ$		
00	0.1275	165
10	0.3032	105
$\bar{1}0$	0.0873	42
01	0.1146	153
$0\bar{1}$	0.1249	153
11	0.2962	72
$\bar{1}\bar{1}$	0.0772	141
$\bar{1}1$	0.2041	130
$1\bar{1}$	0.2370	46
$2\bar{2}$	0.0850	47
02	0.3126	100
$0\bar{2}$	0.4214	76
$\bar{1}2$	0.1374	56
$\bar{1}\bar{2}$	0.1415	76
$3\bar{1}$	0.2513	101
$2\bar{1}$	0.0908	136
mean	0.1791	1599

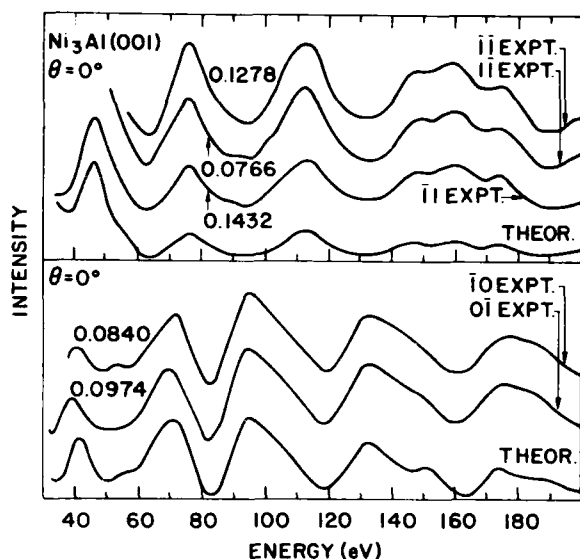
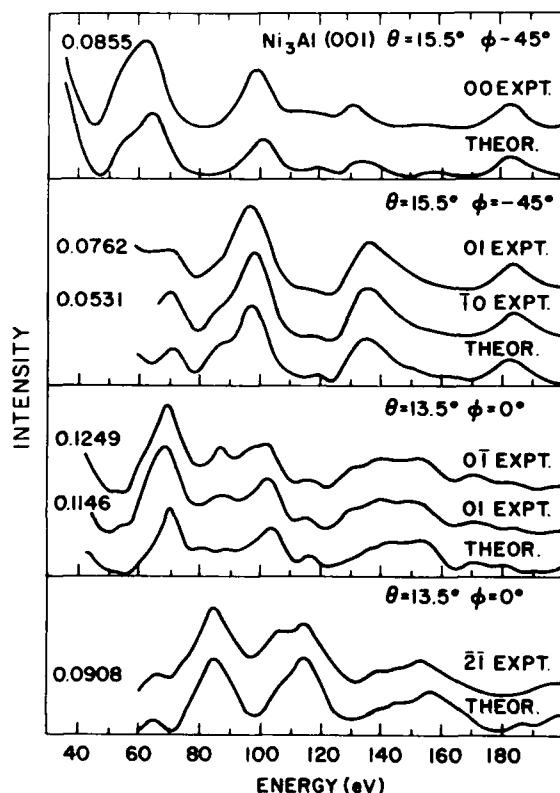


FIG. 3. Examples of best fits for the normal-incidence data.

### III. ANALYSIS

The LEED intensity calculations were done with the dynamical multiple-scattering CHANGE program described elsewhere;<sup>5</sup> 6 phase shifts and 49 beams were used for energies up to 200 eV. The Ni and Al potentials were the band-structure potentials used in earlier studies of Ni and Al surfaces, respectively. The inner potential was chosen initially as  $V_0 = -(10 + 3.5i)$  eV but the real part was

FIG. 4. Examples of best fits for the data at  $\theta = 15.5^\circ$ ,  $\phi = -45^\circ$ , and  $\theta = 13.5^\circ$ ,  $\phi = 0^\circ$ .

treated as an adjustable parameter in the course of the analysis; the final value was  $V_0 = -(13 + 3.5i)$  eV. The initial calculations done with bulklike first interlayer spacing  $d_{12}$  were sufficient to eliminate the 100% Ni termination and to establish the mixed-layer termination.<sup>1</sup> The refinement was carried out only for the latter termination as follows. Changes in  $d_{12}$  from  $-0.2$  to  $+0.2$  Å were combined with changes in  $d_{23}$  from  $-0.15$  to  $+0.05$  Å to fit the normal-incidence data and to build a net of  $r$ -factor values<sup>6</sup> in which a minimum of the  $r$  factor was sought; a minimum was found for  $\Delta d_{12} = -0.049$  Å and  $\Delta d_{23} = 0$ . With the best values of  $d_{12}$  and  $d_{23}$  thus found, the possibility of surface buckling was investigated by allowing Ni and Al atoms in the top layer to be on planes separated by a distance which varied by  $\pm 0.1$  Å. A shallow  $r$ -factor minimum was found for a slight buckling of 0.02 Å (Al atoms up). Then with the structural parameters thus found for the normal-incidence data, the nonnormal-incidence data were introduced into the analysis. First, calculations were made for values of the incident angle  $\theta$  varying by  $\pm 1^\circ$  and  $\pm 2^\circ$  away from the measured value ( $15^\circ$ ). For the two sets with  $\phi = -45^\circ$  and  $\phi = 0^\circ$ ,  $r$ -factor minima were found for  $\theta = 15.5^\circ$  and  $\theta = 13.5^\circ$ , respectively. With the best values of  $\theta$  and  $\phi$ , a

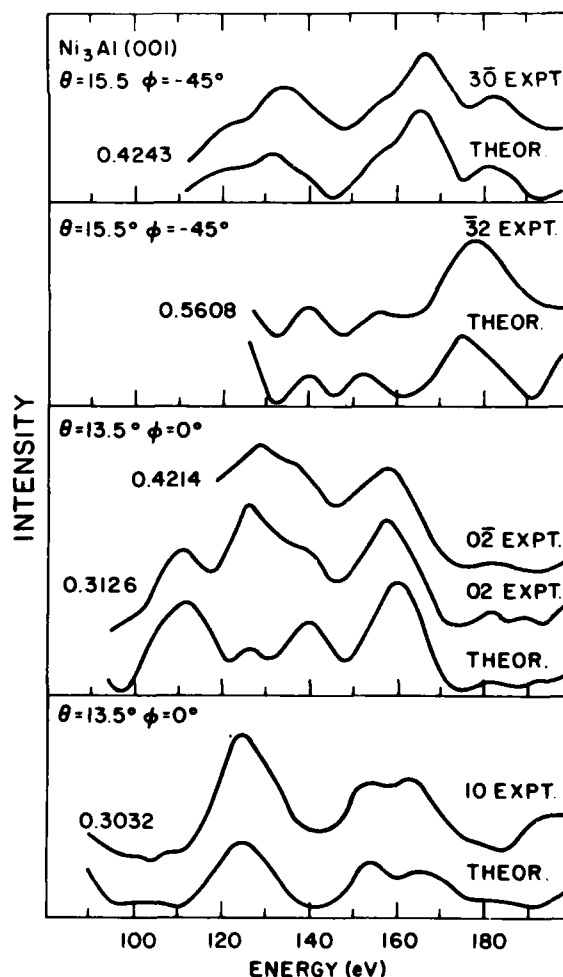


FIG. 5. Examples of worst fits overall.

minimum of the  $r$  factor was sought for values of  $d_{12}$  ranging from  $-0.15$  to  $+0.05$  Å and was found at the same value that optimized the fit at normal incidence. In all cases, the  $r$ -factor minima took into account variations of the real part of the inner potential  $V_0$  as well (these variations correspond to rigid translations of calculated and observed spectra relative to one another<sup>7</sup>).

The final results for the structural parameters were the following: the second interlayer spacing  $d_{23}$  is bulklike (1.78 Å); the first interlayer spacing  $d_{12}$ , defined here as the distance between the second layer (100% Ni) and the plane of Ni atoms in the first layer, is contracted 0.05 Å (or 2.8%) with respect to the bulk value (1.78 Å); the plane of Al atoms in the first layer is moved outwards 0.02 Å. The error bars attached to these numbers are estimated to be about  $\pm 0.03$  Å (see, e.g., Jona *et al.*<sup>8</sup>). Complete documentation of the quality of fit between theory and experiment would involve presentation of 45 calculated and 45 experimental spectra. However, we economize on space by presenting a table with the  $r$  factors of *all* spectra (see Table I) and including only three figures. Figures 3 and 4 show some of the best fits from each of the three sets of data ( $\theta=0^\circ$ ;  $\theta=15.5^\circ$ ,  $\phi=-45^\circ$ ;  $\theta=13.5^\circ$ ,  $\phi=0^\circ$ ) and Fig. 5 depicts five of the worst fits overall. We note that on the whole the agreement between theory and experiment is very good. The mean  $r$  factor is 0.1048 over an energy range of 1613 eV for the normal-incidence data, 0.1854 over 1476 eV for the set at  $\theta=15.5^\circ$ ,  $\phi=-45^\circ$ , and 0.1791 over 1599 eV for the set at  $\theta=13.5^\circ$ ,  $\phi=0^\circ$ .

#### IV. CONCLUSIONS

The LEED intensity analysis of Ni<sub>3</sub>Al{001} described above reveals a rather small contraction of 2.8% of the first interlayer spacing (bulk value 1.78 Å) and a slight buckling of the top layer, the Al atoms being  $0.02 \pm 0.03$  Å outwards from the Ni atoms. The second interlayer spacing is bulklike. We have noted that the stability of the mixed-layer termination is consistent with a first-principles calculation of the cohesive energy<sup>1</sup> and is consistent with the ion-scattering results of Buck *et al.*<sup>9</sup> on the isomorphous Cu<sub>3</sub>Au{001}. However, the structural details found here represent the first such information on the crystallography of Ni<sub>3</sub>Al surfaces and can therefore not be compared with other investigations. Structural studies of alloy surfaces are presently beginning to appear in the literature [NiAl{110} (Ref. 10), CuAl{111} (Ref. 11), and Pt<sub>x</sub>Ni<sub>1-x</sub>{111} (Ref. 12)] but comparisons are premature. Of interest is the fact that on the {110} surface of NiAl, an ordered alloy with the CsCl structure, Davis and Noonan, with LEED analysis, found a mixed surface layer with a large buckling relaxation, the Al atoms being 0.22 Å outwards from the Ni atoms.<sup>10</sup>

#### V. ACKNOWLEDGMENTS

D. S. and F. J. are grateful to the U.S. Office of Naval Research for partial support of this work. Thanks are also due to D. Pearson of the United Technology Research Center for growing the Ni<sub>3</sub>Al ingot from which the sample used in this work was obtained.

<sup>1</sup>D. Sondericker, F. Jona, V. L. Moruzzi, and P. M. Marcus, *Solid State Commun.* **53**, 175 (1985).

<sup>2</sup>The proximity of the energy values of the two AES lines considered here (61 and 68 eV) makes it necessary to define precisely how the ratio  $R_A$  was measured. In the doubly differentiated AES spectrum usually recorded in these studies, the positive excursion of the Al line is obliterated by the Ni line. Thus, for present purposes, the height of the Ni line was measured as usual between the positive and the negative excursions of the Ni line, while the height of the Al line was measured between the positive excursion of the Ni and the negative excursion of the Al line.

<sup>3</sup>F. Jona, J. A. Strozier, Jr., and P. M. Marcus, in *The Structure of Surfaces*, edited by M. A. Van Hove and S. Y. Tong (Springer, Berlin, 1985), p. 92.

<sup>4</sup>F. Jona, *J. Phys. C* **11**, 4271 (1978).

<sup>5</sup>D. W. Jepsen, H. D. Shih, F. Jona, and P. M. Marcus, *Phys.*

*Rev. B* **22**, 814 (1980).

<sup>6</sup>E. Zanazzi and F. Jona, *Surf. Sci.* **62**, 61 (1977).

<sup>7</sup>P. M. Marcus, F. Jona, S. Finch, and H. Bay, *Surf. Sci.* **103**, 141 (1981).

<sup>8</sup>F. Jona, D. Westphal, A. Goldmann, and P. M. Marcus, *J. Phys. C* **16**, 3001 (1983).

<sup>9</sup>T. M. Buck, E. H. Wheatley, and L. Marchut, *Phys. Rev. Lett.* **51**, 43 (1983).

<sup>10</sup>H. L. Davis and J. R. Noonan, *Phys. Rev. Lett.* **54**, 566 (1985).

<sup>11</sup>D. F. Ogletree, M. A. Van Hove, G. A. Somorjai, and R. J. Baird, *Bull. Am. Phys. Soc.* **29**, 222 (1984); *Surf. Sci.* (to be published).

<sup>12</sup>Y. Gauthier, R. Baudoing, Y. Joly, J. Rundgren, J. C. Bertolini, and J. Mollardier, *Europhysics Conference Abstracts*, Vol. 9C (ECOSS-7) (1985), p. 284.



Accession For	
NTIS GRA&I	<input type="checkbox"/>
DTIC TAB	<input type="checkbox"/>
Unannounced	<input type="checkbox"/>
Justification	
By	
Distribution/	
Availability Codes	
Dist	Avail and/or Special
A-1 21	